Electro-polymerized receptor coatings for the quantitative detection of histamine with a catheter-based, diagnostic sensor

Gideon Wackers [a], Peter Cornelis [a], Tristan Putzeys [a,b], Marloes Peeters [c], Jan Tack [d], Freddy Troost [e], Theodor Doll [f], Nicolas Verhaert [b], Patrick Wagner [a*]

[a] Laboratory for Soft Matter and Biophysics, KU Leuven, Celestijnenlaan 200D, B-3001 Leuven, Belgium

[b] Research Group Experimental Oto-rhino-laryngology, KU Leuven, O&N II, Herestraat 49, B-3001 Leuven, Belgium

[c] School of Engineering, Newcastle University, Newcastle upon Tyne, NE1 7RU, United Kingdom

[d] Translational Research in Gastrointestinal Disorders TARGID, O&N I, Herestraat 49, B-3000 Leuven, Belgium

[e] NUTRIM School of Nutrition and Translational Research in Metabolism, Maastricht University, Universiteitsingel 40, NL-6229 ER Maastricht, The Netherlands

[f] Institute of AudioNeuroTechnology VIANNA, Hannover Medical School, Stadt-felddamm 34, D-30625 Hannover, Germany

Author handling the submission:

Drs. Gideon Wackers
KU Leuven, Laboratory for Soft Matter and Biophysics
Celestijnenlaan 200 D
B-3001 Leuven, Belgium

E-mail: Gideon.Wackers@kuleuven.be
Phone: +32 – 16 – 37 78 84

***) Corresponding author:**

Prof. Dr. Patrick Wagner
KU Leuven, Laboratory for Soft Matter and Biophysics
Celestijnenlaan 200 D
B-3001 Leuven, Belgium

E-mail: PatrickHermann.Wagner@kuleuven.be
Phone: +32 – 16 – 32 21 79

Keywords: Biomimetic sensors,
Molecularly imprinted polymers,
Electro-polymerization,
Impedance spectroscopy,
Minimally-invasive diagnostics.

Abstract:

In this article, we report on the development of a catheter-based, biomimetic sensor as a step towards a minimally-invasive diagnostic instrument in the context of functional bowel disorders. Histamine is a key mediator in allergic and inflammatory processes in the small intestines; however, it is a challenge to determine histamine levels at the duodenal mucosa and classical bioreceptors are unsuitable for use in the digestive medium of bowel fluid. Therefore, we have developed molecularly-imprinted polypyrrole coatings for impedimetric sensing electrodes, which enable the quantification of histamine in non-diluted, human bowel fluid in a broad concentration range from 25 nM to 1 μM. The electrodes show negligible cross-sensitivity to histidine as a competitor molecule and, for comparison, we also evaluated the response of non-imprinted- and taurine-imprinted polypyrrole to histamine. Furthermore, using equivalent-circuit modelling, we found that the molecular recognition of histamine by polypyrrole primarily increases the resistive component of the electrode-liquid interface while capacitive effects are negligible. The sensor, integrated into a catheter, measures differentially to correct for non-specific adsorption effects in the complex matrix of bowel fluids and a single triggering frequency is sufficient to determine histamine concentrations. Together, these features are beneficial for real-time diagnostic tests.

Medical background

Irritable bowel syndrome (IBS) is a medical condition that affects 11% of the global population, albeit with variations depending on country, age and sex.[1] The pathophysiology is not well understood and, until date, it has not been possible to identify a common disease mechanism that would be universally present in all IBS patients. The diagnosis is currently based on the so-called Rome IV criteria, which rely on the incidence frequency of typical symptoms such as painful diarrhea, constipation and abdominal hypersensitivity.[2–4] These symptoms alone are often inconclusive and may also relate to other disorders besides IBS. There is increasing evidence that the spectrum of IBS symptoms can have a variety of causes such as disordered gut-brain interactions,[5] atypical food allergies,[6] and a low-level, chronical immune response with mast-cell activation in the mucosa of the small intestines.[7, 8] Mast-cell activation is accompanied by release of the inflammation mediator histamine and recent studies show that down-regulating the mast-cell activity and blocking of histamine receptors by pharmaceuticals can alleviate the symptoms in certain sub-sets of IBS patients.[9, 10] However, mastocytosis disease is also characterized by an increased mast-cell count in the gastrointestinal (GI) tract. While the typical after-meal symptoms in diarrhea-predominant IBS correlate with increased serotonin levels in the blood histamine seems to play no role in this case.[11–13] In the latter case, encouraging therapeutic results have been obtained with a drug that blocks a subtype of serotonin receptors.[14]

In this complex situation, it is desirable to have improved diagnostic methods at hand that allow to distinguish efficiently between IBS and other disorders (causing the same or similar symptoms), and ideally also to classify IBS patients in function of their underlying disease mechanism. This would considerably facilitate to select appropriate, personalized therapy based on pharmaceuticals as mentioned above, or on specific diets that are often high in fibers, or low in carbohydrates, or seek to exclude triggering food items. Assessing the involvement of histamine and food allergens can be done by taking biopsies from the intestinal mucosa and by confocal laser endomicroscopy (CLE), which visualizes swelling after injecting potentially allergenic food items into the mucosa.[15, 16] This means that both methods are invasive and therefore we propose a less invasive solution, being a nasogastric catheter that will eventually allow measuring the concentration of histamine that is released from the mucosa to the lumen of the duodenum. This should enable to evaluate the response to food triggers in real time and directly at the site of interaction. We point out that histamine measurements on stool samples are possible, but not suitable as a diagnostic tool for IBS because of the long transit time

between duodenum and rectum and the histamine produced naturally by the microbiome in the colon.

Considerations on the sensing principle

The aim of measuring time-dependent histamine concentration in the upper intestines, more specifically in the duodenum that is located beneath the stomach and separated from it by the pyloric sphincter, creates boundary conditions regarding the sensing principle and the receptors. Evidently, standard techniques for histamine quantification, ELISA (enzyme-linked immunosorbent assay) testing and mass spectrometry, are not applicable for *in vivo* testing. A hypothetical, wireless sensing device will be propelled by peristaltic bowel movement, facilitating to obtain time-resolved information from the bowel segment of interest. This led us to catheter-based impedance spectroscopy in its non-Faradaic variant (without redox mediators) as proposed earlier, see[17]; fiber-optical surface-plasmon resonance might be another valid alternative.[18] Gravimetric detection with micro-resonators will be affected by the uncontrolled viscosity of bowel fluids while measurements based on heat transfer, employed earlier for quantitative histamine detection as described in[19, 20], can hitherto not function inside the body with its homogeneous temperature of 37 °C.

Regarding the receptors, the choice is limited given the fact that bowel fluid is digestive due to its enzymes while the pH value is usually on the acidic side. The typical pH in the GI tract of healthy young adults ranges from pH 5.4 to 7.5 while extreme values down to pH 3 are documented for functional-dyspepsia patients, partly due to stomach acid leakage.[21, 22] Under these circumstances, antibodies will usually degrade. Enzymes might be more stable and an enzymatic histamine sensor has been reported in literature.[23] However, their selectivity is unclear in case of bowel fluid with its high natural contents of pancreatic enzymes.[24] In principle, histamine-selective aptamers might be useful; however, they became available only very recently and are not yet optimized to function in an acidic pH range.[25, 26] This brings us to the option of molecularly imprinted polymers (MIPs) that are known as selective, synthetic receptors for histamine already since 2010. [27, 28] **Figure 1** illustrates the molecular structure of histamine. After MIP synthesis, the template molecules are usually extracted using organic solvents and strong acids, meaning that the structural integrity of MIP materials does not deteriorate in bowel fluid.

The stability in acidic media was *e.g.* illustrated in our recent work on a catheter-type, impedimetric histamine sensor, which could quantify histamine in the physiologically normal range (5-200 nM).[17] In that specific case, we employed coatings (20 – 30 μm thickness) consisting of MIP micro-powders, synthesized from acrylic-acid (AA) monomers and fixated on titanium wires by using polystyrene as an adhesive. The AA-based MIPs show a consistent binding affinity for histamine from pH 5 to 9, which is an improvement over MIPs made of methacrylic acid (MAA), binding histamine only between pH 7 and 9.[27–29] These pH ranges were calculated with a combinatorial model that considers that binding only takes place if a histamine molecule can establish 1 (maximum 2) hydrogen bridges with its surrounding binding site. We refer to ref.[29] for the mathematical details, which involve the acid-dissociation constants (pK_a values) of the monomers and histamine, which occurs in three different protonation states (His-N, His+, His++), depending on the pH of the medium. As mentioned above, patients suffering from bowel disorders can have an intestinal pH down to 3,[22] where histamine is only present in its His++ form, meaning that AA-based MIPs will not be able to cope with this situation. This suggests that MIP materials might be better for which the histamine recognition does not rely on hydrogen bridges but, instead, on pH-independent interactions such as π-π stacking.[30]

MIP materials allowing for π-π interactions can for instance be synthesized through electro-polymerization from monomers with aromatic ring structures: Well-known examples include PEDOT-PSS (poly(3,4-ethylene-dioxythiophene) polystyrene sulfonate),[31–33] and p-ATP (poly-aminothiophenol),[34] while ref.[35] reviews all recent evolutions up to 2019. In the present work, we chose pyrrole (Py), see **Figure 1**, as a functional monomer for several reasons:

- Pyrrole has been used before to synthesize histamine-sensitive MIP coatings on diamond electrodes, albeit still without a cross-selectivity test towards histidine.[36] Histidine is the precursor of histamine and both have an imidazole ring in common which can interact via π-π stacking.

- Literature is not unanimous, but PPy is widely considered as biocompatible or at least as bio-tolerable.[37–39] The catheter sensor is not a medical implant for which strict biocompatibility requirements would apply, but still the material should not provoke adverse reactions while being placed in the GI tract.

- Impedimetric sensing exploits a concentration-dependent change of the amplitude or phase angle of the complex impedance signal. These changes can be minute for very small target concentrations; therefore, the background impedance of the sensor circuit should be as low as possible to discern these small changes. PPy is a good candidate in this aspect due to its comparatively high electrical conductivity.[22, 40]

Figure 1 illustrates all molecules involved in the present work, together with a scheme of π-π interactions between histamine and the polypyrrole MIP. Clearly, π-π stacking is also possible between histidine and pyrrole, meaning that special attention must go to cross-selectivity testing. Since sensor-based assays on complex media can be compromised by non-specific adsorption, it is common practice to employ differential sensing: The data from a non-functional reference channel serve to correct the sensor output for such contributions that may otherwise be registered as false positives. For sensors based on MIP receptors, non-imprinted polymers (NIPs) have been used frequently as a reference.[20, 29, 41, 44] However, a truly non-imprinted polymer is assumed to be less porous than a MIP coating, which poses questions on the comparability. Therefore, we will not only study the response of "true" NIP electrodes to histamine, but also the response of electrodes coated with taurine-imprinted PPy. As seen in **Figure 1**, taurine and histamine have a similar size and both feature an amino group, while taurine has no aromatic properties.

In view of the purpose of the sensor, there are additional reasons to explore the potential of electro-polymerized MIP coatings: The signal of the previously developed sensor (with AA MIPs) saturated for concentrations higher than 200 nM, which is the upper limit of the physiologically normal range.[17] However, concentrations of 500 – 900 nM have been found earlier in ELISA tests on bowel fluid of IBS patients.[29] To use the histamine level as a diagnostic parameter, a sensor should be able to render also unusually high, pathological values correctly. Here, electro-polymerization has an advantage through its precise control on the thickness of the receptor layer, which allows to adjust the number of available binding sites on an electrode to the diagnostic needs. Furthermore, the process is suitable for serial fabrication and can produce (histamine-) sensitive electrodes in large quantities, all with the same detection range and sensitivity; this is a must for routine diagnostic interventions and cohort studies.

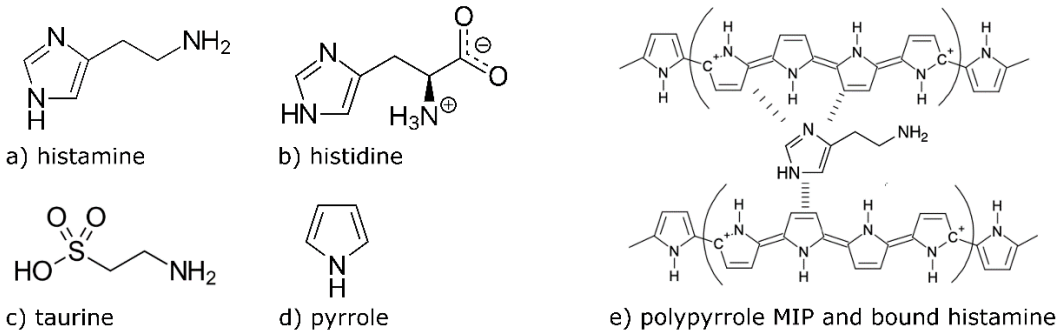

Figure 1: *Molecular structures of* ***a)*** *the target molecule histamine,* ***b)*** *its precursor and main competitor histidine,* ***c)*** *taurine, used as pseudo template for NIP coatings, and* ***d)*** *the pyrrole monomer for MIP synthesis.* ***Panel e)*** *illustrates the two possible binding mechanisms between histamine and the MIP cavity on basis of π-π stacking and hydrogen bonds. Under acidic conditions, hydrogen bonds are not probable due to protonation of the host (pyrrole) and the guest (histamine) while the π-π interaction is pH-independent.*

Materials and Methods

Gastrointestinal catheter and testing setup

Sensors that can quantify histamine selectively have an extremely broad range of potential applications from food-safety analysis to medical diagnostics. In the present work, we focus on the challenging task to detect histamine in real time, directly inside the small intestines of patients suffering from functional bowel disorders. Usually, one would evaluate such sensor first in a suitable animal model, but these do not exist for the conditions of functional dyspepsia and IBS. Hence, in a patients' study, the sensor has to perform "close to perfect" upon first attempt and sensors used on several patients need to have highly reproducible sensitivity. *Vice versa*, a sensor that meets these stringent criteria can rather easily be engineered to measure for instance the histamine contents of food extracts. In a recent publication, see ref.[17] , we have published the design of a catheter with integrated histamine-sensitive electrodes and a testing-setup that mimics the situation inside the duodenum in terms of geometry, temperature, pH and dielectric properties. **Figure 2** shows photographs of the catheter, its sensing compartment (sample chamber) with four wire-shaped electrodes and the testing setup; for technical details and construction drawings, we refer to ref.[17]

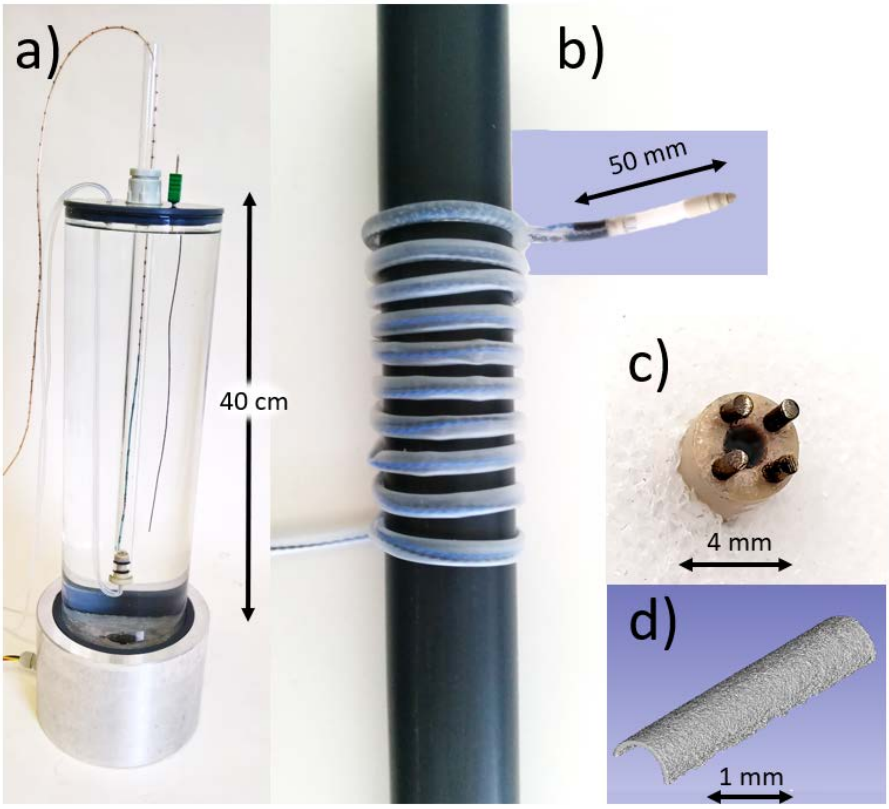

Figure 2: Panel a*) is a photograph of the setup used to keep samples at 37º C in a body-like environment which mimics the insertion of the catheter into a patient. The catheter prototype is shown in* ***b)****, wrapped around a rod, the sample chamber at the distal end is indicated with the 50 mm scale bar.* ***c)*** *Close-up of the coated Ti electrodes with the channel through which air can be injected to remove the protective catheter cap when the catheter is in place and which serves also to aspirate bowel fluid into the sample chamber.* ***d)*** *Optical coherence tomography (OCT) image of a MIP-functionalized electrode, illustrating the smooth and homogeneous morphology of the receptor coating.*

In brief, the catheter is made using a 2-meter long medical-grade silicone tube (Hilltop Products Ltd., Golborne, UK) with 5 mm outer diameter, which is the maximum diameter permitted for catheter insertion by nasogastric intubation. The proximal end of the catheter connects to the impedance analyzer with solderless connectors (DuPont, Mechelen, Belgium) while the distal end features the sample chamber (volume 100 µL) with four embedded titanium wires (0.8 mm Ø, Merck, Overijse, Belgium). The electrodes are kept in place with a centering piece made of PEEK (Polyether ether ketone); this resilient polymer is also used for the rounded tip through which intestinal fluid enters the sample chamber after passing a filter mesh. The electrodes are connected to the proximal end using insulated copper wires that are wound around an aspiration

tube that serves to open the tip (using slight overpressure at the proximal side) and to pull the liquid into the sample chamber (with a slight vacuum). This closure mechanism will prevent stomach fluid from entering the sample chamber before the catheter tip is located inside the duodenum.

Synthesis and characterization of receptor coatings

Prior to functionalization of the titanium-wire electrodes (the length of the PPy-coated part is 3 mm), the native oxide layer was removed by manual polishing with 2000 grit sandpaper, followed by degreasing with 99% pure isopropanol. For electro-polymerization, we used a three-terminal electrochemical cell with the Ti-wires connected sequentially as working electrode(s), a platinum rod as counter electrode, and a Ag/AgCl reference electrode, all together coupled to a PalmSens4 potentiostat (Houten, the Netherlands). The electrolyte (1.0 mL total volume) consisted of 200 µL pyrrole (97% purity, Merck, Overijse, Belgium), mixed with 800 µL of 100 mM aqueous KCl solution based on MilliQ water. Pyrrole requires agitation to properly mix with the KCl solution, which was achieved by vortexing the vial vigorously for 30 seconds. For preparing the histamine-imprinted MIP coatings, the KCl solution was spiked with histamine dichloride (98% purity, Alfa Aesar, Kandel, Germany) to a final concentration of 100 mM of these template molecules. For non-imprinted polymer coatings (NIP), we utilized the same electrolyte fluid, however without spiking the KCl solution with template molecules. When measuring in complex media it is recommended to use a non-imprinted polymer (NIP) reference to acquire information on (bio)fouling and other nonspecific adsorption onto the sensor surface.[17, 19-20, 27-28] Because a NIP electrode should resemble all properties of a MIP electrode as close as possible, except for the selective recognition functionality.

However, since a NIP lacks the presence of template molecules during polymerization, potential morphological differences between MIP- and NIP materials such as their porosity and surface roughness may occur.[42] Therefore, we did not only test a classical NIP coating to correct the sensor signals for non-specific electrode fouling, but also polymer layers that were imprinted with taurine as a “pseudo template”. As seen in **Figure 1c)**, taurine has an amino group similar to histamine, their size is comparable, and their molecular weight is similar with 125.15 g/mol for taurine *vs.* 111.15 g/mol for histamine. To synthesize the taurine-imprinted layers, we used the same solution as described above but added taurine in the same molar ratio as histamine (99%, Merck, Overijse, Belgium). The solutions were purged with nitrogen gas

prior to use and all electro-polymerization reactions were performed at room temperature with 3.0 ± 0.2 mm of the Ti wires dipped into the solutions.

To deposit the polypyrrole layers, we used the same polymerization parameters for all electrode types. The protocol comprised 15 potential cycles in total, each cycle consisting of 950 mV for 60 seconds, followed by 350 mV for 6 seconds with 1 second intervals of zero voltage in between. These parameters were derived from literature and the number of cycles was experimentally optimized to result in complete coverage of the electrodes.[43] A potential of 950 mV will not cause oxidation and/or polymerization of the histamine because these reactions require a potential of minimally 1100 mV and higher, depending on pH.[46] In our specific case the pH of the polymerization solution is above pH 8, where the minimum potential for electrochemical reactions is higher than 1200 mV, hence clearly above the potential used in our experiment. Polymerization was carried out with the four electrodes mounted in the PEEK centering piece; first, we coated the NIP electrode couple and thereafter the MIP electrode couple to avoid unintended contamination of the NIP electrodes with histamine. After deposition of the polymer coatings, the electrodes were rinsed with MilliQ water to remove the thin electrolyte layer with unbound pyrrole and histamine or taurine molecules. Finally, we extracted the template molecules by washing the electrodes in 0.1 M H_2SO_4 for 20 minutes under constant agitation on a shaker, followed by another 20 minutes of washing in 0.1 M NaOH, and a concluding rinsing for 20 minutes in MilliQ to neutralize any remaining acid or base. The combined acid-base washing brings the histamine template molecules into their various protonation states and induces conformational changes which allows them to release from their cavity.[29] The as-prepared electrodes were blown dry with a nitrogen gun and stored in a desiccator until use. Minor differences in baseline impedance of different electrodes are possible due to the manual oxide removal and serial coating of the individual electrodes. Also slight length variations of ± 0.2 mm can cause 10% differences in absolute impedance values. Nevertheless, the baseline impedance of all electrodes was found to be within a reasonable margin from each other.

According to non-destructive imaging by optical coherence tomography (OCT), see **Figure 2d**, the MIP- and NIP coatings on the titanium electrodes had a thickness of 1000 nm (± 400 nm) without any pinholes or other irregularities. The OCT instrument was a Thorlabs Telesto Series OCT device, (Lübeck, Germany) operating at 1300 nm wavelength. The advantage over

the commonly used atomic force microscopy lies in the wider field of view, both laterally and in depth, and in the truly non-destructive layer thickness analysis.

Samples under study

To establish the dose-response curve of the sensor, we performed an initial characterization with phosphate-buffered saline solution (1 × PBS, pH 7.4) as a matrix. The PBS was obtained by dissolving 37.7 g NaCl, 4.4 g Na_2HPO_4, 1 g KH_2PO_4 in five liters of MilliQ water and adjusting the pH to 7.4. This PBS solution was divided into unspiked PBS and a stock solution which was spiked with histamine to a resulting histamine concentration of 10 mM. The pure PBS and the spiked stock were mixed in the appropriate ratios to prepare histamine concentrations starting from 0.5 nM up to 100 µM. For cross-selectivity testing with respect to histidine (see **Figure 1b**), we made the same series of concentrations with histidine, that was purchased from Alfa Aesar, Kandel, Germany, with a purity of 98%.

In view of the intended application, histamine detection in the intestines, we characterized the sensor also with bowel fluids that were aspirated from the duodenum of healthy volunteers and patients at the University Hospitals Leuven and at Maastricht University Medical Center. At both universities, the procedures for sampling the intestinal fluids had been approved in advance by the responsible Medical Ethics Committees. At KU Leuven, the approval has the internal file number s56910 (18/12/2015); for Maastricht University, it is part of a larger study registered in the US National Library of Medicine www.clinicaltrials.gov, ID NCT02018900).

After aspiration, the bowel fluids of several individuals (three or more persons) were mixed to obtain a fluid sample with representative properties, which was stored frozen at –21 °C and thawed for the actual experiments. After thawing, we centrifuged the samples at 7500 rpm for 10 minutes under 7245 g to obtain a clear fluid and determined the pH value, for which we found slight variations between pH 6 and 7. Native histamine, which is present in these samples, was extracted according to the protocol that is documented in earlier work by the authors. [29] To remove the histamine, 10 mg of histamine-MIP micro-powder (AA MIPs) was added for every 3 mL of bowel fluid and the liquid was kept under constant agitation on a shaker for 30 minutes at room temperature to let the particles bind with the histamine molecules. The 10 mg of MIP powder is a ca. 400 fold excess of the quantity that is actually needed to extract the native histamine molecules completely from the bowel fluid samples,

taking into account the binding capacity of these powders, which was determined by analyzing batch-rebinding data with the Freundlich-isotherm model.[29] Here, we made the worst-case assumption that the bowel-fluid samples had a native histamine concentration of 1000 nM, which is the upper limit of what can be expected for IBS patients. Afterwards, the liquid was centrifuged (7500 rpm at 7245 g for five minutes) and the now histamine-loaded particles were discarded. In order to obtain bowel-fluid samples with a series of known histamine concentrations, 10 vol% of histamine-spiked PBS was added to a final concentration range from 2.5 nM to 0.5 mM. These spiked concentrations should be seen as nominal values on which we did no additional reference tests such as ELISA which has an intrinsic uncertainty of ± 50 nM. [29] Within the intestines, there is a continuous release of histamine and histamine breakdown by the enzyme diamine oxidase (DAO) resulting in a certain equilibrium concentration.[47] In the aspirated samples, we have added histamine while evidently no new DAO can be produced as in the intra-intestinal situation where it is continually released from the mucosa. To minimize any potential influence of DAO activity, all samples were kept frozen prior to use as mentioned above and histamine spiking was done immediately before the actual measurements.

Impedance spectroscopy

To test the model catheter in an environment that mimics the gastrointestinal (GI) tract, we performed all impedance measurements using the lower 40 cm of the catheter (as measured from its distal end) inside the body-mimetic testing setup shown in **Figures 2 b, c**. The catheter was hereby located in a glass tube (6 mm inner diameter), that was filled either with histamine-spiked PBS buffer or histamine-spiked intestinal fluid, prepared as described above. By exchanging liquids through the lower end of the glass tube using silicon tubes, 4 mL of fluid was sufficient to obtain a 12 cm high fluid column in the tube with the catheter being in place. We mention this explicitly because bowel fluid is comparatively scarce as one aspiration intervention on a single person typically results in less than 5 mL of liquid. During all experiments, the inner tube was surrounded by a vessel filled with 1 × PBS to mimic the dielectric properties of the body while the temperature of the PBS was actively controlled to maintain 37.0 ^{o}C. For further details on vessel design and temperature regulation we refer to.[17]

A Palmsens4 with MUX8-R2 multiplexer (used also as potentiostat, see above) served as impedance analyzer. Impedance sweeps were performed from 10 Hz to 1 MHz with 10

subdivisions per decade, taking 1 minute per sweep. The excitation voltage of 65 mV is compliant for applications inside the human body. Based on earlier results,[17] we used a symmetrical electrode configuration with electrode couples instead of making a visual distinction between working- and counter electrode. This is beneficial for the signal-to-noise ratio of the resulting impedance spectra and doubles the actual receptor-functionalized surface. When measuring concentration series (both on spiked PBS and spiked bowel fluid), all samples were studied in the order of increasing histamine concentration, starting with the histamine-free liquids. We did not regenerate the electrodes in-between subsequent measurements, which is in principle possible with MIPs as shown by Kupai *et al.*[48] Such treatments with acids and solvents are not feasible when eventually measuring histamine inside the human intestines as a function of time, and retracting and re-inserting the catheter by nasogastric intubation for in-between electrode regeneration during a diagnostic session is not an option.

Results and Discussion

Coating properties

Optical coherence tomography (OCT) was used to evaluate the coating thickness and surface roughness: A layer thickness of 1000 nm with a standard deviation of 400 nm was found both for MIP- and NIP-functionalized electrodes. The surface roughness is comparatively low as visualized in **Figure 2d** and the smooth coating morphology makes it unlikely that larger particles from bowel fluid would stick to the electrode surface once the catheter is actually applied inside the duodenum of patients. All coatings were found to be fully covering the titanium-electrode surfaces without any pinholes or other signs of inhomogeneity.

Impedimetric histamine detection in PBS buffer fluids

The first measurements were performed in PBS buffer to evaluate the sensor response without potentially convoluting the results with effects arising from the complexity of intestinal fluids. The interactions between the sensor coating and the target molecules are expected to become visible in the impedance spectra mainly at frequencies below 10 kHz: Literature on impedimetric small-molecule detection with MIP receptors suggests indeed that frequencies between 100 Hz and 1 kHz result in the highest sensitivity and the lowest limits of detection (LoD).[20, 27, 29, 42] Nevertheless, we probed the complete frequency range from 10 Hz to 1 MHz with histamine-MIP electrodes as shown in the Bode plot of **Figure 3a** for pure PBS and PBS spiked with 1 µM of histamine. The data are taken from a concentration series and 1 µM corresponds to the upper end of the pathophysiological range. It is clearly visible that the

molecular recognition results in a substantial impedance increase at all frequencies, making the selection of an appropriate triggering frequency less critical. Repeating this experiment with a second couple of histamine-imprinted electrodes, now exposed to histidine, shows only a minor increase of the impedance amplitude. This indicates a very good selectivity of the coatings, keeping the similarity of histamine and histidine at the molecular level in mind (see **Figure 1**). For an easier comparison, **Figure 3b** shows the impedimetric response at a fixed frequency, here 158 Hz, throughout the entire concentration range under study. For each concentration, the data are normalized to their respective value in pure PBS, which was taken as 100%. For histamine, the signal increases almost linearly as a function of the logarithm of the concentration up to 10 µM with a slope of 14% per decade; above 10 µM there is a tendency towards saturation. The linearity of the response as a function of the logarithm of the concentration is presumably related to the positive charge of histamine (His+, His++). For histidine, the slope is *ca.* 1.5% per decade, which means that the *imprinting ratio* is 10 to 1.

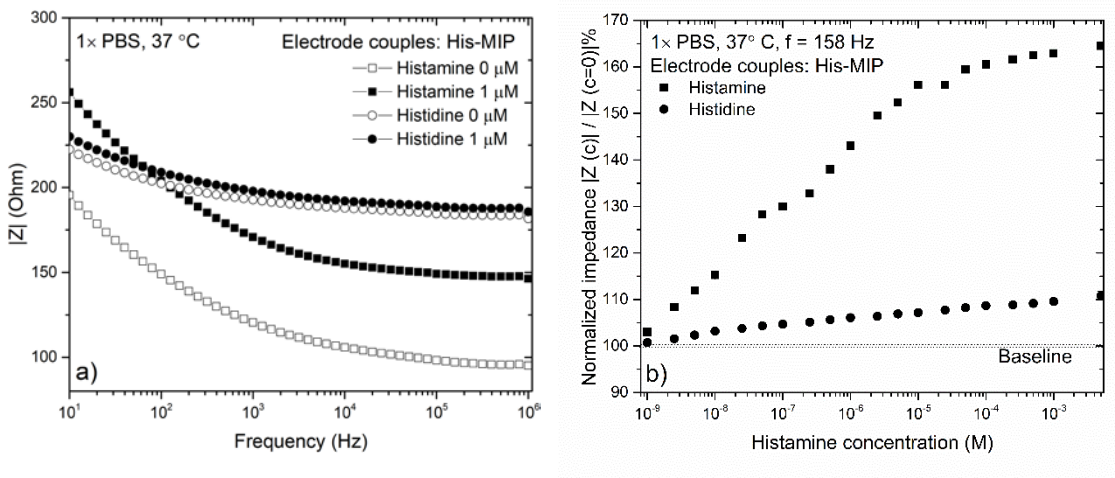

Figure 3: a) *Impedance spectrum of two histamine-sensitive electrode couples in pure PBS buffer (open symbols) and in PBS spiked with respectively 1 µM of histamine (solid boxes) and 1 µM of the competitor histidine (solid dots). The impedance increase due to selective histamine binding is visible throughout the entire spectrum while the response to histidine is far less pronounced.* ***b)*** *Concentration dependence of the impedance increase at a fixed frequency (f = 158 Hz) for all concentrations under study, the 100% baseline corresponds to the impedance amplitude in pure PBS at 158 Hz.*

Figure 4a addresses whether the impedance increase upon exposure to histamine is related to non-specific adsorption by studying an electrode couple that features taurine MIPs, and a second couple with non-imprinted PPy coatings (NIP). The spectra of both electrode sets in

pure PBS are again widely similar and they resemble the spectra of the histamine-imprinted electrodes of **Figure 3a**. Upon spiking with 1 µM histamine, the NIP electrodes display an impedance increase by *ca.* 5 % while the taurine electrodes have no discernible impedance change. This is surprising, given the similarity between taurine and histamine in terms of molecular weight and their amino groups; *vice versa* it indicates that electro-polymerized PPy MIPs can indeed achieve an appreciable level of selectivity. Imprinting with the non-aromatic taurine molecules does not bring about cavities that would allow for histamine recognition, meaning in turn that the π-π interactions do play a role in the binding between histamine and histamine imprinted polypyrrole MIPS. Furthermore, the absolute impedance values of NIP electrodes and taurine MIP electrodes are practically identical, which implies that the potential differences in roughness or porosity cannot be confirmed. An increase in surface area and roughness would reveal itself through lower values of the absolute impedance.

Panel 4b renders the normalized response of the three electrode-coating types (histamine MIP, taurine MIP, NIP) as a function of the histamine concentration at the fixed frequency f = 158 Hz. The taurine MIPs are insensitive to histamine and there is an *imprinting ratio* of again 10 to 1 when comparing the response of the histamine-MIP- and NIP electrodes at concentrations up to 10 µM.

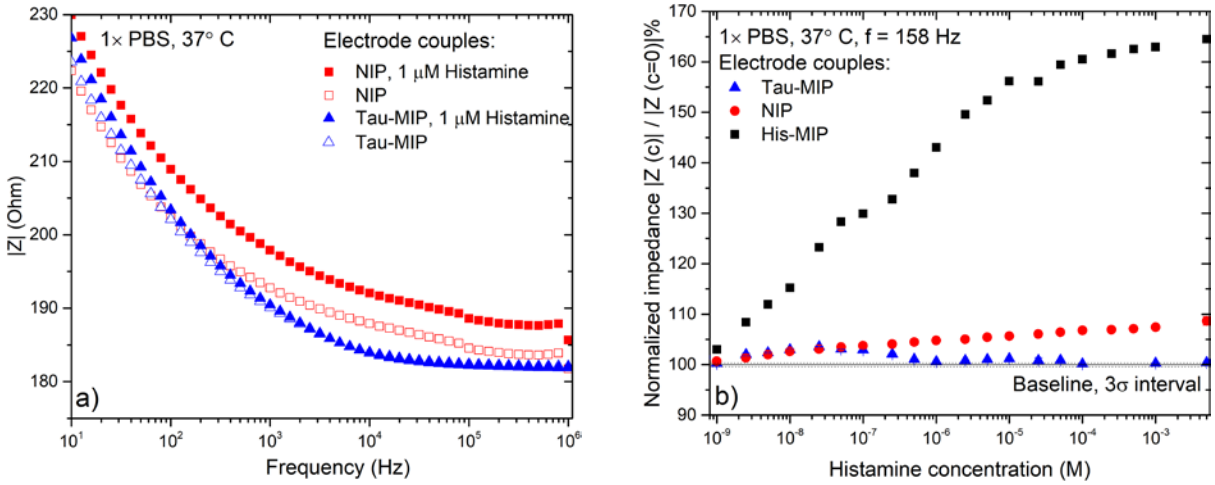

***Figure 4**: **a)** Impedance spectra of an electrode couple with a non-imprinted PPy coating (NIP, open boxes) and a taurine-imprinted electrode couple (Tau-MIP, open triangles) in pure PBS. Exposure to 1 µM histamine causes a slight increase of the impedance amplitude for the NIP electrodes while the taurine-imprinted electrodes show no response (both given as solid symbols). **b)** Change of the normalized impedance at 158 Hz for the entire concentration range in case of the NIP- (red dots) and taurine-imprinted electrodes (blue triangles), the 100%*

*baseline corresponds to pure PBS. The limit of detection with histamine-MIP electrodes is 2.5 nM, this is the lowest measured value for which the signal exceeds the 3σ interval around the baseline (indicated by dotted lines). Comparison with the response of histamine-sensitive electrodes (solid boxes, data from **Figure 3b**) shows that these NIP electrodes respond only weakly and for the taurine-imprinted electrodes it is almost absent.*

Based on these findings, both types of electrode couples (NIPs and taurine MIPs) would qualify as a reference channel for the differential impedance measurements on real bowel fluids that are discussed later. We decided to employ NIP-coated electrodes for this purpose because these electrodes show a minor response to histamine, while not actually binding the target: This way, the signal of the MIP channel does not only correct for electrode fouling, but also for an (hypothetical) impact of unbound histamine on the MIP electrodes. We will see in **Section. 3.4** that this effect is in practice negligibly small. In **Figure 4b** the dotted lines indicate the limit of detection (LoD) of 2.5 nM for histamine in PBS, it was calculated by multiplying the standard deviation σ of the baseline by a factor of 3.

Equivalent-circuit analysis in buffer fluid

To understand the mechanism behind the impedance increase upon binding of histamine to MIP-functionalized electrodes, we analyze the frequency- and concentration dependence of the impedance spectra by equivalent-circuit modelling. **Figure 5a** shows a spectrum obtained with pure PBS and these data are raw, as-measured data (the **Figures 3a** and **4a** show raw data as well). Due to the geometry of the catheter with long wires (2 m), twisted and wound around the aspiration tube, a certain impedance contribution must be expected that we have measured by shunting the sensing electrodes inside the catheter tip. The cable impedance is almost constant with *ca.* 10 Ω up to $f = 10^5$ Hz and shows an upturn for higher frequencies, which suggests an inductive effect. Subtracting the cable impedance from the raw data results in the corrected spectrum of **Figure 5a**. The data for $f > 10^5$ Hz were discarded from further analysis because at this frequency the impedance analyzer changes its internal calibration standard, which can result in errors on the difference signal. For modelling the corrected spectrum, we evaluated a variety of equivalent circuits and the modified Randles circuit, shown in **Figure 5b**, gave the best results in terms of the R^2 value (0.996). Here, R_L is a serial, ohmic resistance of the electrolyte while R_{MIP} and C_{MIP} stand for the resistive and capacitive properties of the receptor coating. W is a Warburg element that represents the possible change of the protonation state of histamine molecules when being in electrical contact with the electrodes.[17] Based on

this circuit, the frequency dependence of the impedance signal is given by **Eq. 1**, which takes into account the real- and the imaginary impedance components (j stands for the imaginary unit).

$$Z_{tot}(\omega) = \left(j\omega C_{MIP} + \frac{1}{R_{MIP}}\right)^{-1} + \frac{W(1-j)}{\sqrt{\omega}} + R_S \qquad \textbf{Equation 1}$$

Translating **Eq. 1** back to the absolute $|Z|$ values results in the fit curves shown in **Figure 5c** exemplarily for pure PBS and for PBS with spiked histamine concentrations of 100 nM, 1 µM, and 10 µM. Depending on the concentration, R^2 is between 0.994 and 0.997. For comparison, we considered also circuits with *RC* in parallel, *R*-*W* in series, and a non-modified Randles cell, hence without the Warburg element. The data analysis is given in the **Supporting Information SI 1** and, depending on the model, the goodness factor R^2 of these fits varies between 0.760 (with two circuit components) and 0.940 (three circuit components).

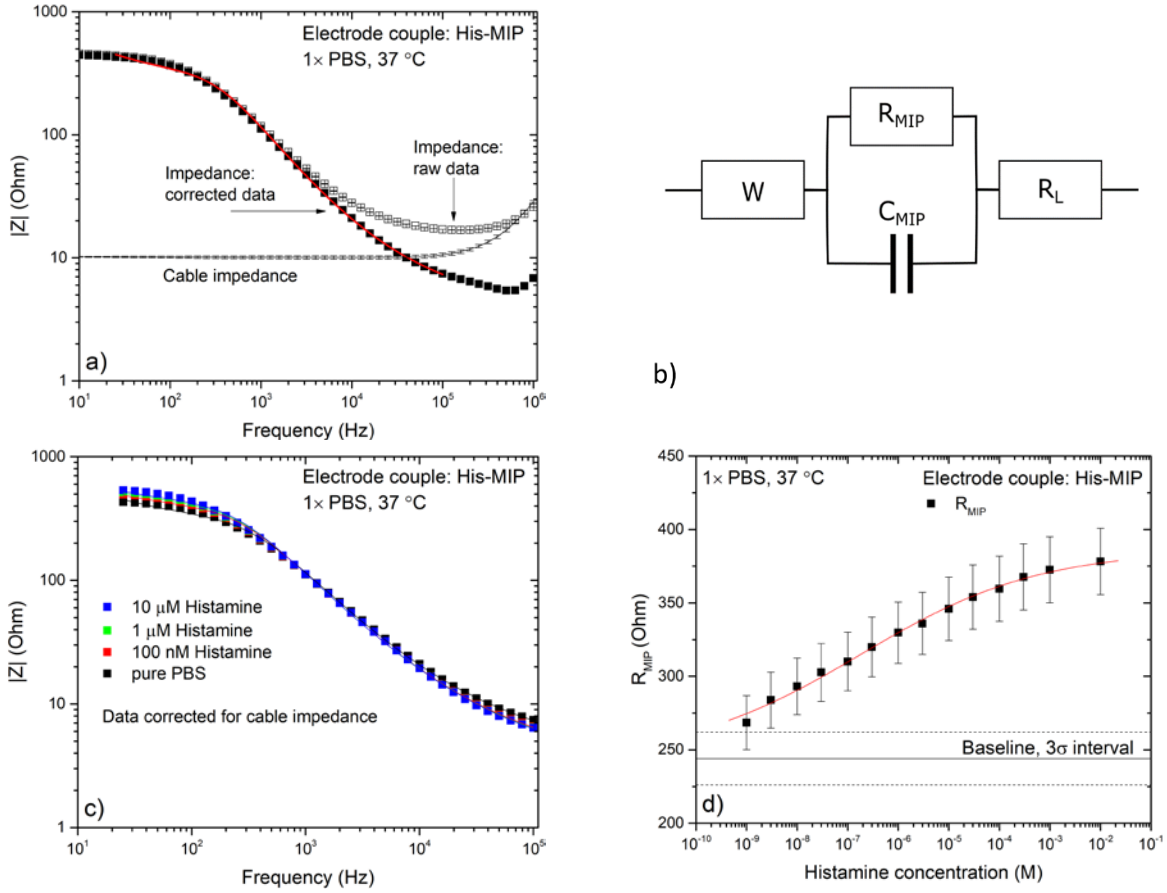

Figure 5: *Panel* ***a)*** *As-measured impedance spectrum of a MIP-functionalized electrode couple in pure PBS (open boxes), cable impedance, and the data corrected for the cable contribution (solid boxes). The solid line is a fit curve based on* ***Eq. 1****.* ***b)*** *Equivalent circuit for modelling*

the corrected impedance spectra in pure and histamine-spiked PBS: W is a Warburg element, C_{MIP} and R_{MIP} represent the capacitive and resistive properties of the electrode-liquid interface, R_L is the resistance of the liquid. ***c)*** *Corrected and fitted spectra for pure PBS and after spiking with the indicated histamine concentrations.* ***d)*** *Concentration dependence of the resistive component R_{MIP}, the error bars represent the uncertainty on the fitted R_{MIP} values. The solid line is a guide to the eye, the baseline corresponds to non-spiked PBS.*

The parameter that displays the clearest correlation with the histamine concentration is the interface resistance R_{MIP} as seen in **Figure 5d**. The three other parameters, W, C_{MIP} and $R_{L,}$ vary only weakly or insignificantly with the histamine concentration, which is illustrated in the **Supporting Information SI 2**. The algorithm to determine the four-parameter set for all concentrations is documented in **SI 2** as well.

Hence, the data suggest that the resistive component plays a key role in signal generation, which agrees with earlier findings on electrodes functionalized with MIPs made of acrylic-acid powers.[17] There are also literature data that point to capacitive effects as being relevant for the impedance increase upon binding of target molecules by MIP coatings.[20] This was interpreted in the sense that target molecules replace water molecules inside the binding cavities and this will change the effective dielectric properties of the MIP layer. In the present case however, the absolute change of the fitted C_{MIP} values is not significant when moving from pure PBS to the highest histamine concentrations. We point out that the results of equivalent-circuit modelling should be seen as indicative, but not as being conclusive. A full understanding can possibly be achieved by dielectric spectroscopy with a high enough resolution to obtain information at the scale of the binding cavities.

Dose-response analysis with intestinal fluids

As described above, native histamine present in bowel-fluid samples had first been extracted with a proven protocol, and then known histamine doses were added to nominal resulting concentrations from 25 nM to 10 μM. This corresponds to the range from the normal level to *ca.* the tenfold of what is expected in a pathophysiological (IBS) condition. Irrespective of spiking, all samples consisted still for 90% of bowel fluid, which is by definition a highly complex medium: Duodenal fluid contains a plethora of food-, fat-, and protein residues, digestive enzymes, bile salts, mucus and other components that will attack or foul the receptor coatings on the electrodes. Differential sensing is the method of choice to correct for non-

specific adsorption (electrode fouling), which would otherwise be registered as a false-positive impedance increase. The method assumes that fouling happens equivalently at the active channel with MIP-functionalized electrodes and at the "passive channel" with a NIP-coated electrode couple. **Figure 6a** shows the concentration-dependent increase of the impedance signal at two different frequencies (158 and 252 Hz) for a MIP-electrode couple, respectively for a NIP couple. All values are normalized for easier comparison, the 100% level corresponds to the impedance amplitude of each electrode pair in histamine-free bowel fluid. Even without normalization, both electrode couples have a similar impedance value, in this case 332 Ω for the MIP couple and 358 Ω for the NIP couple, both at 158 Hz.

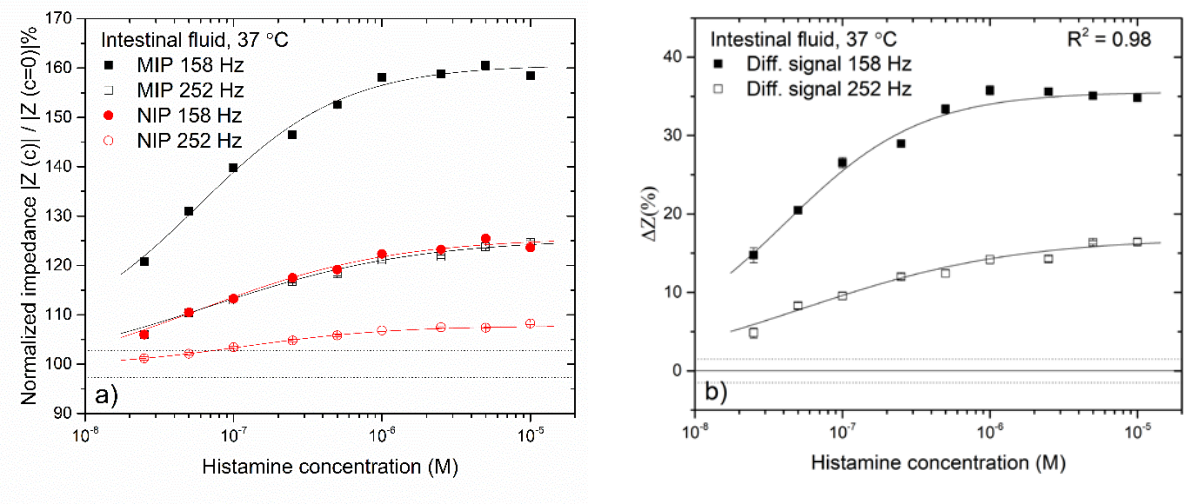

Figure 6: a) *Normalized impedance of a MIP-electrode couple (solid symbols) and a NIP couple (open symbols) upon exposure to histamine-spiked bowel fluid at f = 158 Hz and 252 Hz. The baseline represents the signal for histamine-free bowel fluid and the corresponding 3σ interval. Error bars on the data (smaller than symbol size) are calculated from 5 impedance sweeps per concentration, lines are a guide to the eye.* ***b)*** *Difference signal ΔZ(%) between the MIP- and the NIP-electrode pair for 158 Hz (solid boxes) and 252 Hz (open symbols). The solid line through the data was calculated with the dose-response function* ***Eq. 2****. The LoD is below 25 nM and the dynamic range is up to 1 μM, i.e. the upper pathophysiological regime.*

Looking *e.g.* at the data for the MIP couple at 158 Hz, the relative impedance increase at a given concentration, for example at 1 μM histamine, is slightly higher than in case of PBS spiked with the same concentration (see **Figure 3b**). For the NIP couple, this holds in the same way, suggesting that there is indeed a progressive fouling effect when the electrodes are in contact with bowel fluid. **Figure 6b** shows the difference signal *ΔZ*% between the active- (MIP) and the passive (NIP) channel for both considered frequencies; these signals reflect the

true impedance change due to selective histamine recognition, free of false-positive contributions due to fouling and also due to non-specific histamine adsorption. It is clearly visible that the change of $\Delta Z\%$ as a function of the concentration is more pronounced for 158 Hz than for 252 Hz, suggesting that lower frequencies allow in tendency for a more sensitive detection. The differential curve can be modelled with the dose-response fit function of **Eq. 2**, which is based on the sigmoid dose-response theory and embedded in the Origin software package.[45]

$$\Delta Z\%\,(C) = \Delta Z\%_{\,min} + \frac{\Delta Z\%_{\,max} - \Delta Z\%_{\,min}}{1 + 10^{(\log(d50) - \log(C))}} \qquad \textbf{Equation 2}$$

Since we look at difference signals, it is evident that $\Delta Z\%_{\,min} = 0$ while the fit parameter $\Delta Z\%_{max}$ is the signal under saturation, d_{50} is the concentration at which the difference signal has 50% of the saturation value. In contrast to PBS with a quantifiable concentration range up to 10 µM (see **Figure 4b)**, signal saturation in bowel fluid starts already slightly above 1 µM. We assume that this is related to the fouling effect because fouling reduces the accessibility of the binding sites (at least a fraction thereof) for target molecules. However, this result is a considerable improvement over the 200 nM obtained earlier with acrylic-acid MIPs and, from the diagnostic perspective, it is hardly expected to find values above 1 µM in the duodenum of IBS patients. Should it become necessary to quantify higher concentrations, one can opt *e.g.* for thicker MIP coatings and/or modify the template-monomer ratio to increase the number of binding sites. The limit of detection in bowel fluid was found to be below the lowest measured concentration of 25 nM histamine. As mentioned above, there might be a breakdown of histamine due to enzymatic conversion by DAO. If DAO is active during the measurements, it would mean that the real histamine concentrations are potentially lower than the nominal values and, vice versa, the effect size of the impedimetric measurement underestimates the intrinsic value for a given , absolute concentration. For future applications on patients however, this plays not a role as the concentration is in a dynamic equilibrium between histamine release and breakdown by DAO.

Interestingly, there was no visual degradation of the MIP layers after exposure to bowel fluid for almost three hours, being the typical duration of measuring a concentration series such shown in **Figure 6**, which includes stabilization and regular medium exchange. As mentioned, we did not wash or regenerate the electrodes when moving from a given concentration to the next-higher one. The chemical and structural resilience of the PPy-based electrode coatings for hours in digestive bowel fluid at body temperature is in any case encouraging towards utilizing

these electrodes also in extended diagnostic sessions to study *e.g.* the stimulus-induced histamine release as a function of time.

Summary and Conclusions

In this work, we have reported on the development of a catheter-based impedimetric sensor that will eventually allow quantification and monitoring of the histamine concentration in the human duodenum. This "catheter sensor" offers the perspective to become a diagnostic tool in the context of functional bowel disorders. Although known as "irritable bowel syndrome IBS", there is in current understanding neither a single disease mechanism that would be present in all patients nor a universally applicable therapy that would benefit all IBS patients. However, the catheter sensor should facilitate identifying the subgroup of IBS patients in which the symptoms go along with chronically or temporarily elevated histamine levels. This holds for the rare disorder of mastocytosis and for the frequently observed atypical food allergies in which certain food items induce intestinal histamine discharge. The existing diagnostic techniques for these conditions are invasive and involve for instance biopsies from the intestinal mucosa. In contrast, the catheter sensor is only minimally invasive because it will pick up the histamine release from the mucosa passively as a chemical signal without stimulating it. An extension of the sensing method towards other molecular biomarkers in the duodenum is possible.

The challenge of intestinal sensing lies not only in getting the sensor to the point of interest, but also in the complexity of bowel fluid as a matrix with digestive properties and an unpredictable pH value. Molecularly imprinted polymers are resilient under such conditions and the MIP-based electrode coatings used in our experiments have proven stable for three hours in contact with pure bowel fluid. This is certainly long enough for intestinal diagnostic interventions with nasogastric catheters, taking three hours at most to limit the burden for the patient. To avoid complications through a pH-dependent binding affinity for histamine, as observed in prior work, we have chosen for polypyrrole as MIP material, deposited by electro-polymerization on wire-type titanium electrodes. The binding interaction with histamine is based on pH-independent π–π stacking between aromatic rings, which is an imidazole group in case of histamine. The same group is present in the competitor histidine, which suggests substantial cross-sensitivity. As seen from the data however, the response of the electrodes towards histidine is small and comparable with electrodes featuring non-imprinted polypyrrole coatings. A further benefit of electro-polymerization is its intrinsic suitability for the batch

synthesis of sensing electrodes with highly reproducible characteristics, which is a precondition for the reliability of the intended diagnostic application.

The measured sensing parameter is the concentration-dependent impedance increase: According to equivalent-circuit modelling and taking the cable impedance into account, this is mainly due to the resistive component of the electrode-liquid interface. Capacitive effects, if any, seem to be of minor importance. For establishing the dose-response curves, a full-spectrum analysis is however not necessary because the absolute impedance value at a fixed trigger frequency already provides sufficient information on concentrations. This in turn means that the readout electronics can in principle be kept at a basic level. Furthermore, the data were not compromised by electronic noise even without the use of electromagnetic shielding for the two-meter long wires, running through the catheter, which can act as an antenna. Together, these are important advantages when deploying the catheter sensor in future in a clinical setting. Regarding the limit of detection, we measured an LoD of 2.5 nM in phosphate buffer while it is *ca.* 25 nM in non-diluted bowel fluid obtained from several patients by aspiration. In case of bowel fluid, this LoD is at the lower side of the physiologically normal range and, most importantly, there is still a one-to-one correspondence between the sensor signal and the concentration in the regime up to 1 μM. This is a substantial improvement over previous results, in which the signal saturated already around 200 nM, meaning that the sensor could not differentiate between concentrations within the pathological regime. In case of diagnosed IBS patients, values up to *circa* 1 μM can be expected and are documented in literature. In the present work, we have studied the characteristics of the catheter sensor not only on real bowel fluid but, to advance the technology towards its purpose, in a testing setup that mimics the intra-body situation in terms of geometry, temperature, and dielectric properties. Since there are no suitable laboratory-animal models for functional gastrointestinal disorders, a novel diagnostic device requires especially stringent *in vitro* testing and optimization; exploratory studies on healthy volunteers are the next step to take.

Associated content

Supporting Information: The Supporting Information is available free of charge at https://pubs.acs.org/doi/to-be-determined

Contents: Data modelling of impedance spectra with alternative equivalent circuits (PDF)

Notes: The authors declare no competing financial interest.

Acknowledgements

We kindly acknowledge financial support by the Research Foundation Flanders FWO for the project G.0B25.14N "Monitoring of gut functions and inflammation processes with biomimetic sensors based on molecularly imprinted polymers". T. Putzeys acknowledges FWO funding through the postdoctoral fellowship 12Y69.19N while N. Verhaert is supported in part by the FWO clinical investigators grant 18048.16N. The contribution by M. Peeters became possible by the EPSRC New Investigator Award EP/R029296/2. P. Cornelis and P. Wagner thank for internal KU Leuven funding via the project C32/18/025, that enabled starting up molecular-imprinting research within the Laboratory for Soft Matter and Biophysics. Stimulating scientific discussions with Prof. T. Junkers (Monash University, Australia) are kindly appreciated.

References

1) Canavan, C.; West, J.; Card, T. The epidemiology of irritable bowel syndrome. *Clinical Epidemiology* **2014**, *6*, 71 – 80.

2) Drossman, D.A. Functional gastrointestinal disorders: History, pathophysiology, clinical features, and Rome IV. *Gastroenterology* **2016**, *150*, 1262 – 1279.

3) Schmulson, M.J.; Drossman, D.A. What is new in Rome IV. *Journal of Neurogastroenterology and Motility* **2018**, *23* (2), 151 – 163.

4) Rome Foundation Webpage https://theromefoundation.org/, accessed on May 31, 2020.

5) Drossman, D.A.; Tack, J.; Ford, A.C.; Szigethy, E.; Törnblom, H.; Van Oudenhove, L. Neuromodulators for functional gastrointestinal disorders (disorders of gut – brain interaction): A Rome foundation working team report. *Gastroenterology* **2018**, *154* (4), 1140 – 1171.

6) Fritscher-Ravens, A.; Pflaum, T.; Mösinger, M.; Ruchay, Z.; Röcken, C.; Milla, P.J.; Das, M.; Böttner, M.; Wedel, T.; Schuppan, D.; Many patients with irritable bowel syndrome have atypical food allergies not associated with immunoglobulin E. *Gastroenterology* **2019**, *157* (1), 109 – 118.

7) Barbara, G.; Stanghellini, V.; De Giorgio, R.; Cremon, C.; Cottrell, G.S.; Santini, D.; Pasquinelli, G.; Morselli-Labate, A.M.; Grady, E.F.; Bunnett, N.W.; Collins, S.M.; Corinaldesi, R. Activated mast cells in proximity to colonic nerves correlate with abdominal pain in irritable bowel syndrome. *Gastroenterology* **2004**, *126*, 693 – 702.

8) Wood, J.D. Histamine, mast cells, and the enteric nervous system in the irritable bowel syndrome, enteritis, and food allergies. *Gut* **2016**, *55*, 445 – 447.

9) Lobo, B.; Ramos, L.; Martínez, C.; Guilarte, M.; González-Castro, A. M.; Alonso-Cotoner, C.; Pigrau, M.; de Torres, I.; Rodiño-Janeiro, B. K.; Salvo-Romero, E.; Fortea, M.; Pardo-Camacho, C.; Guagnozzi, D.; Azpiroz, F.; Santos, J.; Vicario, M. Downregulation of mucosal mast cell activation and immune response in diarrhoea-irritable bowel syndrome by oral disodium cromoglycate: A pilot study. *United European Gastroenterology Journal* **2017**, *5* (6), 887 – 897.

10) Wouters, M.M.; Balemans, D.; Van Wanrooy, S.; Dooley, J.; Cibert-Goton, V.; Alpizar, Y.A.; Valdez-Morales, E.E.; Nasser, Y.; Van Veldhoven, P.P.; Vanbrabant, W.; Van der Merwe, S.; Mols, R.; Ghesquière, B.; Cirillo, C.; Kortekaas, I.; Carmeliet, P.; Peetermans, W.E.; Vermeire, S.; Rutgeerts, P.; Augustijns, P.; Hellings, P.W.; Belmans, A.; Vanner, S.; Bulmer, D.C.; Talavera, K.; Vanden Berghe, P.; Liston, A.; Boeckxstaens, G.E. Histamine receptor H1-mediated sensitization of TRPV1 mediates visceral hypersensitivity and symptoms in patients with irritable bowel syndrome. *Gastroenterology* **2016**, *150* (4), 875 – 887.

11) Doyle, L.A.; Sepehr, G.J.; Hamilton, M.J.; Akin, C.; Castells, M.C.; Hornick, J.L. A clinico-pathologic study of 24 cases of systemic mastocytosis involving the gastrointestinal tract and assessment of mucosal mast cell density in irritable bowel syndrome and asymptomatic patients. *American Journal of Surgical Pathology* **2014**, *38* (6), 832 – 843.

12) Atkinson, W.; Lockhart, S.; Whorwell, P.J.; Keevil, B.; Houghton, L.A. Altered 5-hydroxy-tryptamine signaling in patients with constipation- and diarrhea-predominant irritable bowel syndrome. *Gastroenterology* **2006**, 130 (1), 34 – 43.

13) Houghton, L.A., Atkinson, W.; Whitaker, R.P.; Whorwell, P.J.; Rimmer, M.J. Increased platelet depleted plasma 5-hydroxytryptamine concentration following meal ingestion in symptomatic female subjects with diarrhoea predominant irritable bowel syndrome. *Gut* **2003**, *52* (5), 663 – 670.

14) Garsed, K.; Chernova, J.; Hastings, M.; Lam, C.; Marciani, L.; Singh, G.; 1, Henry, A.; Hall, I.; Whorwell, P.; Spiller, R. A randomised trial of ondansetron for the treatment of irritable bowel syndrome with diarrhea. *Gut* **2014**, *63* (10), 1617 – 1625.

15) Fritscher-Ravens, A.; Schuppan, D.; Ellrichmann, M.; Schoch, S.; Röcken, C.; Brasch, J.; Bethge, J.; Böttner, M.; Klose, J.; Milla, P.J. Confocal endomicroscopy shows food-associated changes in the intestinal mucosa of patients with irritable bowel syndrome. *Gastroenterology* **2014**, *147* (5), 1012 – 1020.e4.

16) Vanheel, H.; Vicario, M.; Vanuytsel, T.; Van Oudenhove, L.; Martinez, C.; Keita, A.V.; Pardon, N.; Santos, J.; Soderholm, J.D.; Tack, J.; Farre, R. Impaired duodenal mucosal integrity and low-grade inflammation in functional dyspepsia. *Gut* **2014**, *63* (2), 262 – 271.

17) Wackers, G.; Putzeys, T.; Peeters, M.; Van de Cauter, L.; Cornelis, P.; Wübbenhorst, M.; Tack, J.; Troost, F.; Verhaert, N.; Doll, T.; Wagner, P. Towards a catheter-based impedimetric sensor for the assessment of intestinal histamine levels in IBS patients. *Biosensors and Bioelectronics* **2020**, *158*, art. no. 112152, 10 pp.

18) Loyez, M.; Larrieu, J.C.; Chevineau, S.; Remmelink, M.; Leduc, D.; Bondue, B.; Lambert, P.; Devière, J.; Wattiez, R.; Caucheteur, C. In situ cancer diagnosis through online plasmonics. *Biosensors and Bioelectronics* **2019**, *131*, 104 – 112.

19) Peeters, M.; Csipai, P.; Geerets, B.; Weustenraed, A.; van Grinsven, B.; Thoelen, R.; Gruber, J.; De Ceuninck, W.; Cleij, T.J.; Troost, F.J.; Wagner, P.; Heat-transfer based detection of L-nicotine, histamine, and serotonin using molecularly imprinted polymers as biomimetic receptors. *Analytical and Bioanalytical Chemistry* **2013**, *405* (20), 6453 – 6460.

20) Peeters, M.; Troost, F.J.; van Grinsven, B.; Horemans, F.; Alenus, J.; Murib, M.S.; Keszthelyi, D.; Ethirajan, A.; Thoelen, R.; Cleij, T.J.; Wagner, P. MIP-based biomimetic sensor for the electronic detection of serotonin in human blood plasma. *Sensors and Actuators B – Chemical* **2012**, *171 – 172*, 602–610.

21) Dressman, J.B.; Berardi, R.R.; Dermentzoglou, L.C.; Russell, T.L.; Schmaltz, S.; Barnett, J.; Jarvenpaa, K. Upper gastrointestinal (GI) pH in young, healthy men and women. *Pharmaceutical Research* **1990**, *7* (7), 756 – 761.

22) Lee, K.J.; Demarchi, B.; Demedts, I.; Sifrim, D.; Raeymaekers, P.; Tack, J. A pilot study on duodenal acid exposure and its relationship to symptoms in functional dyspepsia with prominent nausea, *American Journal of Gastroenterology* **2004**, *99* (9), 1765 – 1773.

23) Torre, R.; Costa-Rama, E.; Lopes, P.; Nouws, H.P.A.; Delerue-Matos, C. Amperometric enzyme sensor for the rapid determination of histamine. *Analytical Methods* **2019**, *11*, 264 – 1269.

24) Worning, H.; Müllertz, S. pH and pancreatic enzymes in the human duodenum during digestion of a standard meal. *Scandinavian Journal of Gastroenterology* **1966**, *1* (4), 268 – 283.

25) Mairal Lerga, T.; Jauset-Rubio, M.; Skouridou, V.; Bashammakh, A.S.; El-Shahawi, M.S.; Alyoubi, A.O.; O'Sullivan, C.K. High affinity aptamer for the detection of the biogenic amine histamine. *Analytical Chemistry* **2019**, *91* (11), 7104 – 7111.

26) Ho, L.S.J.; Fogel, R.; Limson, J.L. Generation and screening of histamine-specific aptamers for application in a novel impedimetric aptamer-based sensor. *Talanta* **2020**, *208*, art. no. 120474, 12 pp.

27) Bongaers, E.; Alenus, J.; Horemans, F.; Weustenraed, A.; Lutsen, L.; Vanderzande, D.; Cleij, T.J.; Troost, F.J.; Brummer, R.J.; Wagner, P. A MIP-based biomimetic sensor for the impedimetric detection of histamine in different pH environments. *Physica Status Solidi A* **2010**, *207* (4), 837 – 843.

28) Horemans, F.; Alenus, J.; Bongaers, E.; Weustenraed, A.; Thoelen, R.; Duchateau, J.; Lutsen, L.; Vanderzande, D.; Wagner, P.; Cleij, T.J. MIP-based sensor platforms for the detection of histamine in the nano- and micromolar range in aqueous media. *Sensors and Actuators B – Chemical* **2010**, *148* (2), 392 – 398.

29) Peeters, M.; Troost, F.J.; Mingels, R.H.G.; Welsch, T.; van Grinsven, B.; Vranken, T.; Ingebrandt, S.; Thoelen, R.; Cleij, T.J.; Wagner, P. Impedimetric detection of histamine in bowel fluids using synthetic receptors with pH-optimized binding characteristics. *Analytical Chemistry* **2013**, *85* (3), 1475 – 1483.

30) Chen, T.; Li, M.; Liu, J. π−π Stacking interaction: A nondestructive and facile means in material engineering for bioapplications. *Crystal Growth & Design* **2018**, *18*, 2765 – 2783.

31) Cardoso, A.R.; de Sá, M.H.; Goreti F. Sales, M. An impedimetric molecularly-imprinted biosensor for Interleukin-1β determination, prepared by in-situ electropolymerization on carbon screen-printed electrodes. *Bioelectrochemistry* **2019**, *30*, art. no. 107297, 9 pp.

32) Schweiger, B.; Kim, J.; Jun K. Y.; Ulbricht, M. Electropolymerized molecularly imprinted polypyrrole film for sensing of clofibric acid. *Sensors* **2015**, *15*, 4870 – 4889.

33) Ermiş, N.; Tınkılıç, N. Preparation of molecularly imprınted polypyrrole modified gold electrode for determination of tyrosine in biological samples. *International Journal of Electrochemical Science* **2017**, *13*, 2286 – 2298.

34) Nguy, T.P.; Phi, T.V.; Tram, D.T.N., Eersels, K.; Wagner, P.; Truong T.N.L. Development of an impedimetric sensor for the label-free detection of the amino acid sarcosine with molecularly imprinted polymer receptors. *Sensors and Actuators B: Chemical* **2017**, *246*, 461 – 470.

35) Crapnell, R.D.; Hudson, A.; Foster, C.W.; Eersels, K.; van Grinsven, B.; Cleij, T.J.; Banks, C.E.; Peeters, M. Recent advances in electrosynthesized molecularly imprinted polymer sensing platforms for bioanalyte detection. *Sensors* **2019**, *19* (5), art. no. 1204, 28 pp.

36) Ratautaite, V.; Nesladek, M.; Ramanaviciene, A.; Baleviciute, L.; Ramanavicius, A. Evaluation of histamine imprinted polypyrrole deposited on boron doped nanocrystalline diamond. *Electroanalysis* **2014**, *26*, 2458 – 2464.

37) Ramanaviciene, A.; Kausaite, A.; Tautkus, S.; Ramanavicius, A. Biocompatibility of polypyrrole particles: an in-vivo-study in mice. *Journal of Pharmacy and Pharmacology* **2007**, *59*, 311 – 315.

38) Fahlgren, A.; Bratengeier, C.; Gelmi, A.; Semeins, C.M.; Klein-Nulend, J.; Jager, E.W.H.; Bakker, A.D. Biocompatibility of polypyrrole with human primary osteoblasts and the effect of dopants. *PLoS ONE* **2015**, *10* (7), art. no. e0134023, 17 pp.

39) Akkermans, O.; Spronck, M.; Kluskens, T.; Offerein, F.; Saralidze, K.; Aarts, J.; Keshaniyan, P.; Steen Redeker, E.; Diliën, H. van Grinsven, B.; Cleij, T.J. Application of electrodeposited piezo-resistive polypyrrole for a pressure-sensitive bruxism sensor. *Physica Status Solidi (A)* **2016**, *213* (6), 1505 – 1509.

40) Kremers, T.; Menzel, N.; Freitag, F.; Laaf, D.; Heine, V.; Elling, L.; Schnakenberg, U. Electrochemical impedance spectroscopy using interdigitated gold–polypyrrole electrode combination. *Physica Status Solidi A* **2020**, 217, 9 pp.

41) Thoelen, R.; Vansweevelt, R.; Duchateau, J.; Horemans, F.; D'Haen, J.; Lutsen, L.; Vanderzande, D.; Ameloot, M.; vandeVen, M.; Cleij, T.J.; Wagner, P. A MIP-based impedimetric sensor for the detection of low-MW molecules. *Biosensors & Bioelectronics* **2008**, *23* (6), 913 – 918.

42) Alizadeh, T.; Akhoundian, M. A novel potentiometric sensor for promethazine based on a molecularly imprinted polymer (MIP): The role of MIP structure on the sensor performance, *Electrochimica Acta* **2010**, 55 (10), 3477–3485.

43) Ramanaviciene, A.; Ramanavicius, A. Molecularly imprinted polypyrrole-based synthetic receptor for direct detection of bovine leukemia virus glycoproteins, *Biosensors & Bioelectronics* **2004**, *20* (6), 1076–1082.

44) Ramakers, G.; Wackers, G.; Trouillet, V.; Welle, A.; Wagner, P.; Junkers, T. Laser-grafted molecularly imprinted polymers for the detection of histamine from organocatalyzed atom transfer radical polymerization. *Macromolecules* **2019**, *52* (6), 2304 – 2313.

45) Yadav, S.K. Development and monitoring. *International Journal of Environmental Science* **2013**, 4 (3), 77 – 80.

46) Lee, S.T.; Jill, B. Venton mechanism of histamine oxidation and electropolymerization at carbon electrodes. *Analytical Chemistry* **2019**, 91 (13), 8366 – 8373.

47) Bieganski, T.; Kusche, J.; Lorenz, W.; Hesterberg, H.; Stahlknecht C.d.; Feussner, K.D.; Distribution and properties of human intestinal diamine oxidase and its relevance for the histamine catabolism. *Biochimica et Biopysica Acta* **1983**, 756, 196 – 203.

48) Kupai, J.; Razali, M.; Buyuktiryaki S.; Kecili, R.; Szekely, G.; Long-term stability and reusability of molecularly imprinted polymers. *Polymer Chemistry* **2016**, 8, 666 – 673.